Fishing under the Radar: Illuminating Compliance with China's Annual Fishing Moratorium

Björn Bos*

January 28, 2025

Abstract

This paper evaluates the world's largest fishing ban, the annual fishing moratorium in China, and explores its compliance. We start by estimating the reduction in fishing effort due to the ban. We use vessel broadcast positions and fishing boat detections from nighttime lights and find reductions in fishing activity by up to 90 percent. We then explore characteristics of non-complying vessels and how they respond to the policy: Fishers catch more during evenings and nights, they disable vessel broadcast devices, and we observe more transshipment events. Finally, we find that attractive income opportunities during the ban hamper compliance.

Keywords: Fisheries, Conservation Policy, Regulations, Compliance, Nighttime lights
JEL: C80, Q22, Q28, K42

*University of Hamburg, Department of Economics, Von-Melle-Park 5, 20146 Hamburg, Germany. bjoern.bos@uni-hamburg.de.

doi:10.3368/le.101.3.022824-0019R1

1 Introduction

Marine fisheries are an important source of food security and employment, and provide security for many livelihoods (OECD, 2020). In 2016, the average person consumed 10.7 kg of marine fish and fisheries employed more than 40 million people globally (FAO, 2018). Despite their economic and ecological importance, recent estimates suggest that 53 percent of all fisheries are overfished and that fishing pressure is too high in 63 percent of them (Costello et al., 2016).[1] For managed fisheries and those with a scientific stock assessment, however, the abundance of fish stocks has been increasing on average during the past two decades (Hilborn et al., 2020). This emphasizes the need for fisheries management and regulation to maintain fish stocks at acceptable levels.

Fishing bans are a widely used command-and-control policy instrument to manage and regulate fisheries. This paper focuses on the annual fishing ban in China, as an important example of such a policy, and evaluates its compliance. To rebuild its overexploited fish stocks, China, the world's largest producer of fish, implemented an annual fishing moratorium in 1995. This ban has been expanded in recent years and prohibits any fishing of marine stocks for 3.5–4.5 months in the entire Chinese Exclusive Economic Zone (EEZ). However, the effectiveness of this ban is compromised by illegal, unreported, and unregulated (IUU) fishing. Agnew et al. (2009), for example, estimate that 33 percent of the catches in the whole Northwest Pacific are illegal, unreported, and do not comply with regulations. Even globally, IUU fishing represents a major threat to livelihoods, such that the UN Social Development Goals explicitly aim their end (UN, 2015, Goal 14.4). Besides concerns about conservation efforts, the fight against IUU fishing is further motivated by its linkages to criminal behavior, human rights abuses (McDonald et al., 2021; Sumaila et al., 2020; Tickler et al., 2018), and international conflicts (Park et al., 2020; Spijkers et al., 2019). However, observing and characterizing IUU fishing to improve resource management, fish stock assessments, regulations, and enforcement presents a challenge.

This paper addresses this challenge. We start by estimating the reduction of fishing activity due to the ban using data from vessel broadcast positions and boat detections from nighttime lights. This data also allows us to identify apparent fishing activity during the ban.[2] We then explore the characteristics and locations of non-complying fishing vessels and conduct a detailed analysis of fishers' margins of behavior during the ban. We explore how fishers avoid detection, how they land illicit catches, and document how income opportunities hamper compliance with the policy. Understanding the incentives fishers face, how they respond to regulation, and which vessels are more likely to non-comply, helps in designing better policies to ultimately improve conservation efforts.

To measure fishing activity, we rely on estimates of fishing activity that were identified by different means and largely for different vessels. On the one hand, we use the predicted fishing effort in hours per square kilometer based on vessel broadcast positions from the automatic identification system (AIS) (Kroodsma et al., 2018). As vessels may not be equipped with AIS devices and as fishers can manipulate those devices, we also rely on a second measure of fishing activity: The predicted locations of fishing boats based on nighttime lights of the Visible Infrared Imaging Radiometer Suite (VIIRS) (Elvidge et al., 2015). To attract fish and to increase their harvest, many Asian fishers targeting squid and tuna attach bright lights to their boats to illuminate the surrounding water (Elvidge et al., 2015; Park et al., 2020). While these lights are easily observed from the sky, we can identify those fishers with nighttime satellite observations.

To estimate the reduction in fishing activity due to the policy, we use a fixed-effects estimation strategy. To this end, we construct a panel dataset with the daily fishing activity in each management zone and the weekly fishing activity in spatial grid cells with a resolution of 0.25°. We identify the ban's effect through the staggered introduction and lift of the ban in each management zone and then compare the estimated reductions in fishing activities between data sources, management zones, years, and gear types.

Our results show that fishing activity as measured by vessel broadcast positions suggests a reduction of 90 percent fishing activity during the ban.Nighttime lights confirm a significant reduction in fishing activity due to the ban, but only decrease by 48 percent on average. This suggests that the ban is effective in reducing fishing effort, but that considerable heterogeneities in reduction levels exist. We document several heterogeneities across vessel and gear types, as well as space. We find, for example, the largest reduction of fishing activity from trawlers with the AIS data and the least reductions from vessels targeting squid and tuna with the VIIRS data. In addition, we observe more apparent fishing activity in areas close to neighboring EEZs.

We observe that fishers adjust their time to catch during the ban and fish more during evening and nighttime hours. We also find evidence that fishers seem to disable AIS devices when they illegally fish during the ban and find suggestive evidence that transshipment events occur more often during the ban. The latter is a practice to offload catch to refrigerated cargo vessels that can then land catches (cf. Miller et al., 2018). Finally, we find evidence that an increase in income opportunities, as measured by good fishing conditions during the ban, increases non-compliance.

This paper contributes to several strands of the literature. First, it contributes to studies focusing on the compliance behavior of fishers (e.g., Cabral et al., 2018; Diekert et al., 2021; Drupp et al., 2019; FAO, 2018; Nøstbakken, 2008; Vollaard and Kastoryano, 2023; Watson and Pauly, 2001). The state of common-pool resources is of particular interest for a sustainable stock management. However, the open access to these resources and costly monitoring render it hard to assess the true level of compliance. Previous studies, for example, focus on fishers' truth-telling to regulators (Drupp et al., 2019) or the validity of catch records reported to international organizations (FAO, 2018; Watson and Pauly, 2001). What we know from these studies is that fishers, but also regulators, tend to misreport private information on their actual catches. By using remotely sensed data, we must not rely on reported catch data for our analysis.

And second, we contribute to the economic literature using nighttime lights to infer economic activity (Burke et al., 2020; Donaldson and Storeygard, 2016; Henderson et al., 2012; Jain, 2020). In many applications, nighttime lights on land are used to infer economic activity. We shift our focus to lights at sea and estimate economic activity by fishers which recently became more feasible and popular (for other applications see, for example, Cabral et al., 2018; Englander, 2019; Park et al., 2020).

Related studies have identified and mapped the global extent of fishing and industrial activities using AIS, VIIRS, and synthetic-aperture radar (SAR) data (e.g., Elvidge et al., 2015; Kroodsma et al., 2018; Paolo et al., 2024). Based on such remotely sensed data, the Northwest Pacific has been identified as one key hotspot for IUU fishing (e.g., Oozeki et al., 2018; Park et al., 2020; Welch et al., 2022). To obscure IUU fishing, fishing vessels often offload catch to refrigerated cargo vessels (Miller et al., 2018), disable AIS devices (Welch et al., 2022), and often change vessel identities (Park et al., 2023). A common conclusion from those studies is that more regulated areas, along with better management and enforcement, could improve the state of fisheries (cf. Seto et al., 2023). This study tests this hypothesis and evaluates the effectiveness of the world's largest fishing ban, taking dark fishing vessels into account. Most closely related are Kroodsma et al. (2018) and Paolo et al. (2024) who illustrate the level of AIS fishing effort during the ban and show that China's distant water fleet often travels to other areas such as North Korea during the ban. In addition, Yuan (2023) estimates the reduction of VIIRS boat detections around the start and end of the ban and explores spatial spillovers. Compared to those studies, we not only examine and reveal intended reductions in fishing activity, but we also explore unintended adaptive behaviors. Our analysis first synthesizes the reduction of fishing activity inside the Chinese EEZ in a common estimation framework and employs a variety of robust estimation strategies to provide analytical results. On top of that, we explore the characteristics of non-complying vessels and document several behavioral responses of non-complying fishers.

Our results provide important insights for marine regulators, international fishery organizations, and enforcement agencies. First, we document and highlight heterogeneities in the reduction in fishing activity due to the policy. Although there are substantial reductions in fishing activity on average, targeted enforcement efforts towards specific vessels, gear types, and areas could be promising to reduce remaining non-compliance. Second, insights from the AIS system, on which many regulators rely, should be interpreted with caution and may present a too-optimistic image if fishers manipulate their devices. Remote sensing technologies, such as fishing boat detections from nighttime lights, could complement traditional vessel monitoring systems. They allow for cheaper regulatory costs and could thereby allow for better resource recovery (Riekhof and Noack, 2022). And finally, regulators may want to focus on and target practices that facilitate and support fishing during the ban such as transshipment.

2 Background information

China is the largest producer of fish worldwide (FAO, 2018). Its fishing industry employs more than 18 million people, and its marine capture fishery production harvests more than 14 million tons of fish. China's fishing fleet covers more than 730,000 vessels, and more than 468,000 of these are motorized. Although most motorized vessels are smaller than 12 meters, 61,000 are between 12–24 meters, and 36,000 are over 24 meters (China Fishery Statistical Yearbook, 2020).

To promote food security and economic growth, China encouraged the development of its marine fisheries by promoting its fishing sector and privatizing its fishing vessels in the mid-1980s. These policies led to an extraordinary growth of the fishery sector such that China became the largest fish producer worldwide in the early 1990s (Cao et al., 2017). However, this massive growth and intense fishing effort resulted in the over-exploitation of fish stocks and marine ecosystems. In addition, coastal reclamations and the dumping of waste and emissions into the ocean led to further stress on marine ecosystems and environmental degradation (Lu et al., 2019). Besides many minor reforms, the most important marine policy has been the introduction of an annual fishing ban in 1995, which is also known as the seasonal moratorium on marine fishing (Cao et al., 2017). The fishing ban aims to reduce overall fishing pressure.

Initially, China's annual fishing ban prohibited fishing by all vessels for 2.5–3 months during summer in the Bohai, Yellow, and East China Seas. Due to increasing fishing pressure and further stress on the ecosystems, the ban's scope has been gradually extended both temporarily and spatially. Today, it covers the whole Chinese EEZ and lasts for 3.5–4.5 months, depending on the management zone (see Table A1 in the Appendix for the period in each zone and Figure A1 for the border of each zone). Two single-species fisheries in provincial waters are exempted from the ban as their fishing seasons highly overlap with the ban. These fisheries are, however, managed with other regulations, such as a total allowable catch system. In addition, since 2017, any type of fishing gear aside from fishing tackles is allowed in them (Su et al., 2020). Chinese fishers can receive subsidies to compensate for their lost income, but the size of subsidies seems limited as the annual income share from fishery-related subsidies is less than 4 percent on average (cf. Table A2 in the Appendix.)

The wide-ranging spatial coverage of more than 965,000 square kilometers, the extensive time duration, and the strict enforcement for all fishing vessels are particular features of this policy.

To the best of our knowledge, there is only one similar fishing ban in Bangladesh covering a whole EEZ for several months. Otherwise, fisheries regulators often impose seasonal closures for smaller areas, impose technological constraints on the fishing gear, reduce seasons for specific species, or introduce property rights such as individual transferable quotas (Grainger and Parker, 2013; Stavins, 2011).

The fact that fishing is completely prohibited makes it, in principle, easy for regulators and econometricians to detect non-compliance. As all fishing operations are prohibited, we can treat any fishing activity inside the Chinese EEZ during the ban as a violation. For other restrictions, this is often difficult. When confronted with data on their vessel positions, fishers can often argue that they used the proper gear or only caught allowed species. And in a similar vein, local fish vendors often circumvent enforcement, making it difficult to infer compliance from fish markets (Gonzalez-Lira and Mobarak, 2021). By focusing directly on fishing activity at sea, we try to get as close as possible to the true level of compliance.

To enforce its regulations, Chinese law enforcement inspects, among others, fishing vessels and monitors trade from wholesalers. According to the Ministry of Agriculture (2020), more than 180,000 boats were dispatched in 2019, and more than 3,000 tons of illegal catch were confiscated. Among a list of ten exemplary violations that were made public, five have been subject to violations of the annual fishing ban. Violators who illegally fished, or who have been involved in the purchase or sale of illegally caught fish, were often caught on sea and in ports. Fines ranged from 10,000 to 1.5 million Yuan, fishing vessels were seized, and some violators were brought to prison, which is in line with the United Nations Convention on the Law of the Sea (UN, 1982, Article 73). The enforcement level, however, is often viewed as insufficient, leading to seemingly widespread non-compliance (Cao et al., 2017) and a limited impact of this policy for the recovery of fish stocks (Shen and Heino, 2014).

3 Data

We use daily estimates of fishing activity between January 2013 and December 2019 from two independent remotely sensed data sources:[3] vessel broadcast positions from the AIS system and nighttime lights featuring fishing vessels. Both datasets measure fishing activity by different means and largely for different vessels. Vessel broadcast positions cover vessels with various gear types, and fishing activity throughout the day, but can be prone to manipulation. Nighttime lights, instead, do not require the use of an AIS device, but are only informative for fishing vessels targeting squid and tuna during the night.[4]

For our analysis, we construct two panel datasets with different spatial and temporal resolutions. For our primary dataset, the zone sample, we aggregate fishing activity for each day and management zone. This ensures sufficient variation in the level of fishing activity and enables us to quantify the reduction in fishing activity on a spatial basis most relevant for policymakers. In addition, we construct a grid sample with a resolution of 0.25 degrees. The grid sample contains the aggregated fishing activity for each week and grid cell and allows us to analyze the effect of local environmental conditions on local reductions in fishing activity.

3.1 AIS fishing effort

We use data from Kroodsma et al. (2018) who predict the daily level of fishing effort from AIS signals. In particular, they use fishing vessels' broadcast positions from the AIS system to estimate the number of fishing hours per square kilometer at a resolution of 0.01 degrees.

The AIS system was introduced to prevent collisions at sea, and its signals inform others about the location of the vessel, its speed, and its turning angle. Vessels that are actively fishing often behave in predictive and specific movements. For example, they often have low speed and many changes in directions (De Souza et al., 2016). Hence, Kroodsma et al. (2018) use these observed movements as an input for machine learning algorithms to detect fishing activity and to estimate the time that vessels are actively fishing at a given location.

Since 2012, Chinese fishing vessels that engage in offshore fishing have been required to install and use a vessel position monitoring system. The ship position data is used for approving subsidies and monitoring regulation (Ministry of Agriculture, 2012). While AIS is one applicable vessel position monitoring system, China also permits other systems, such as the state-run BeiDou navigation satellite system, and subsidizes the installation of AIS devices (Ministry of Agriculture, 2013). As a result, around 57 percent of the active motorized fishing vessels with a length of more than 24 meters and 36 percent of those between 12–24 meters in China are equipped with AIS (cf. Kroodsma et al., 2018, Table S4).

In Figure 1a, we show the total AIS fishing effort in 2019 for our study area. While we observe fishing activity in many places, there are several areas with no information on fishing activity. The reasons for the white spots are manifold and reflect the disadvantages of the AIS data (McCauley et al., 2016). The most prominent reason is the weak AIS satellite reception quality in South East Asia which is only partly compensated with terrestrial AIS receivers along the Chinese coastline due to their limited range (Taconet et al., 2019). Other reasons include that vessels may not be equipped with AIS devices and that AIS signals are prone to manipulation. Fishers, for example, can turn them off and disappear from the radar (Hsu et al., 2019; Park et al., 2020). Or, they can manipulate their devices and broadcast fake positions to hide their actual position. To overcome these issues, we use a second measure of fishing activity.

[Insert Figure 1 around here]

3.2 VIIRS boat detections

We also use data from Elvidge et al. (2015) on VIIRS boat detections that use VIIRS satellite images during the night to identify fishing boats. Especially fishers that target squid fish and tuna use lights to attract catches during the night. Together these species make up 10.2 percent of the annual landings in China (cf. Table A4). Fishers targeting these species attach powerful lights to their vessels and illuminate the water around them. As these lights are very bright and some vessels carry several hundreds of them, they can be observed from sky and inform us of fishing activity.[5]

In Figure 2, we show an example of an image taken by the VIIRS satellite and the corresponding VIIRS boat detections at the Gulf of Tonkin. While nighttime lights on land often represent cities and infrastructure, many nighttime lights on water are classified as fishing boats and indicate fishing activity. The boat detection algorithm considers cloud cover and the sharpness of light spikes to ensure correct classifications (Elvidge et al., 2015).

[Insert Figure 2 around here]

In Figure 1b, we show the total number of VIIRS boat detections in 2019 for our study area. Compared to the AIS fishing effort in Figure 1a, the VIIRS boat detections uncover many fishing locations that have been "invisible" before, such as at the Vietnamese coast and the east coast of North Korea.

Nighttime lights have several advantages for measuring fishing activity. First, they are available on a global scale and have a high spatial and temporal resolution. This makes monitoring of large areas easier. Second, we can observe fishing boats regardless of whether they are equipped with AIS devices. And third, nighttime lights are more robust to the manipulation of fishers. Fishers who engage in illegal fishing might turn off their tracking devices to disappear from the radar, but turning off their lights would directly reduce their fishing productivity. In addition, these lights are only visible within sight or once a night with some delay due to the satellite image processing. Thus, regulators often have not monitored nighttime lights in near-real time and fishers have been less likely to be detected with those lights during our study period. As a result, it is more costly for fishers to avoid their detection with nighttime lights and the satellite images are less prone to manipulation.[6] We, therefore, argue that VIIRS boat detections can be more reliable than AIS signals in situations where fishers have an incentive to manipulate their AIS devices, such as during fishing bans or in foreign jurisdictions.

A caveat of the VIIRS boat detections is, however, their sensitivity to moon illumination (Elvidge et al., 2015, 2017). The boat detection algorithm works best in low-light situations like during new moon, but it only detects a limited number of boats on bright nights. The underlying problem is that moonlight can cause variations in the brightness of clouds, making it difficult to identify fishing boats. This can result in measurement errors in our dependent variable and can potentially lead to biased estimates (Jain, 2020). We address this concern in two ways. First, we compare the number of VIIRS boat detections on nights with low and high moon illumination and its correlation with the AIS fishing activity in Figure A2 in the Appendix. Although boat detections are lower during nights with high moon illumination, their correlation with the AIS fishing activity is similar. Hence, the relative level of VIIRS boat detections on bright nights is as informative about fishing activity as on dark nights. Second, we control for moon illumination in our regression analysis by adding it as an independent variable that can affect the number of detected boats.

3.3 Environmental conditions data

Finally, we include daily observations of environmental conditions from the MODIS Aqua Ocean Color Data by NASA (2018). This data includes information on the sea surface temperature, chlorophyll-a concentration, and the phytoplankton absorption coefficient at 443 nm (Aph). The latter two measures are common proxies for the level of phytoplankton abundance (see for example Axbard, 2016; Flückiger and Ludwig, 2015). As phytoplankton is the basis of the ocean's food web, it covaries with the abundance of fish stocks, and we use it to determine good fishing conditions. For the grid sample, we use the sum of the daily phytoplankton absorption coefficients as the weekly phytoplankton abundance unless otherwise stated. Due to cloud cover, spatial gaps between satellite overpasses, and other conditions, several values are missing in the daily environmental conditions. We impute these missing values by rolling forward their last value. This affects around 6 percent of observations for the sea-surface temperature and 17 percent of observations for the chlorophyll-a and phytoplankton absorption coefficient. We also winsorize the observations at the 95 percentile to control for outliers.

3.4 Descriptive statistics

In Figure 3, we depict the timeline of both fishing activity measures in the North Yellow Sea. The AIS fishing effort is generally low during winter and increases in spring. At the introduction of the fishing ban, we observe sharp reductions in fishing activity. And after the ban, we observe sharp increases, which then flatten again during autumn. The timeline of the VIIRS boat detections shows a similar trend but with a higher cyclical variation due to the lunar cycle. Despite its noisier pattern, we also observe the highest number of VIIRS boat detections during autumn, as in the AIS data. The average levels of fishing activity are significantly lower during ban periods than outside the ban, but some fishing activity seems to remain.[7]

[Insert Figure 3 around here]

We provide descriptive statistics of the zone sample in Table 1. According to the AIS data, fishers spend an average of 29,000 hours per day in the first management zone, and 12,000 hours of those are spent fishing. 48 percent of the AIS fishing effort is estimated to come from trawlers, 28 percent from boats using fixed gear, 2 percent from dredge fishing boats, and 21 percent from boats for which an exact fishing gear could not be inferred. From the VIIRS data, we observe 323 fishing boat detections on an average night in the first management zone. While a boat detection indicates fishing activity in an area of 742m $\times$ 742m, this number represents a lower bound of the actual number of boats. Because if multiple boats are located in the same area, there would still be just a single boat detection.

[Insert Table 1 around here]

4 Estimation strategy

We estimate the reduction of fishing activity in response to the fishing ban with a two-way fixed-effects model, a time-series model, and an event-study model. Our preferred model is the two-way fixed effect model, as it is flexible enough to exploit treatment variation between time and space simultaneously. However, it requires strong identification assumptions, and we will point out potential concerns below. The time-series model and event-study model provide evidence from alternative estimation strategies but also share some of those identification assumptions.

Under full compliance and without detection avoidance behavior by fishers, we would expect a reduction of fishing activity by 100 percent. With noncompliance, however, fishing activity would decrease significantly less than 100 percent and if fishers avoid detection, we may overestimate the reduction in fishing activity due to the ban.

Fixed-effects model: We use the exogenous and staggered start and end of the fishing ban to identify the ban's effect with a two-way fixed effects model. The ban periods are exogenous and independent of local fishing efforts and fishing conditions as they are predefined by the Chinese Ministry of Agriculture and fixed for several years. Hence, we compare fishing activity in areas where the ban is in force with areas where the ban is out of force on a given day. Our fixed-effects specification reads as follows:

$$\ln(y^d_{tz}) = \alpha_0 + \beta \mathrm{Ban}_{tz} + \gamma_1 \mathrm{Moon}_t + \gamma_2 \mathrm{Moon}^2_t + \eta \mathbf{X}_{tz} + \mu \mathbf{T}_t + \alpha_{1i} + \epsilon_{tz} \tag{1}$$

where y^d_{tz} indicates the fishing activity y on day t in management zone z as indicated by dataset d (either AIS or VIIRS).[8] Ban_{tz} is a binary dummy variable equal to one if the fishing ban is in force on a given day in a given zone. Moon_t captures the moon illumination in lux as it is an important factor in the boat detection algorithm that explains part of the variation in the daily number of boat detections. The vector $\mathbf{X}_{tz}$ includes a set of additional variables to control for environmental conditions and time-fixed effects. In particular, we include the daily mean sea-surface temperature, chlorophyll-a concentration, and the phytoplankton absorption coefficient (Aph). Motivated by previous research (Kroodsma et al., 2018), we also include weekday fixed effects and a dummy for public holidays to control for local cultural events. In addition, $\mathbf{T}_t$ includes year-fixed effects and the linear and quadratic Julian day to capture time trends during the year. As the fishing ban is always and everywhere in place in June and July, month-fixed effects would capture some of the ban's effect. Hence, we do not include them in our baseline specifications, but report them as a robustness check in Table A12. Finally, α_i captures management-zone fixed effects and ϵ_{tz} any residuals.

Our main coefficient of interest is β, which indicates the reduction in fishing activity due to the ban. To this end, our estimation exploits variation in fishing activity at the start and end of the ban in May, June, August, and September. As our sample covers multiple years with various iterations where the fishing ban starts and ends for a given management zone, β does not allow us to differentiate between the change in fishing activity at the start and end of the ban. Instead, β reflects a weighted average of all changes in fishing activity at the start and end of the ban between all possible two-group and two-period DiD estimates (Goodman-Bacon, 2021).[9] As we use a logarithmic transformation of the fishing activity (y^d_{tz}), we report transformed coefficients (i.e., $\exp(\beta) - 1$) and confidence intervals. Multiplying these by 100 allows for an interpretation in percentage changes.

In our fixed-effects estimations using the zone sample, we cluster standard errors on the management zone level to control for correlations within management zones and for heteroskedasticity. As we only have a few clusters, we calculate them using a Wild clustered bootstrap approach with 500 bootstrap iterations if not stated otherwise (Cameron et al., 2008). As spatial correlation can be problematic for a sample with a fine spatial resolution, we use Conley (1999, 2008) standard errors for estimations using the grid sample. This controls for the fact that fishing effort can correlate between neighboring grid cells. To this end, we allow for a spatial and temporal bandwidth of 1,000 kilometers and 20 weeks.

Assumptions and Limitations: The fixed-effects identification strategy rests on a few assumptions and violations can challenge the validity of our empirical results. In particular, we must assume no temporal reallocation, stable unit treatment value (SUTVA), a common trend, and a homogeneous and constant treatment effect. Except for the assumption of no temporal reallocation, we provide tests and checks for each of them.

First, the assumption of no temporal reallocation requires that fishers do not bring forward or postpone their catches around the ban period. While ecological conditions and temporal variation in the abundance of fish species limit such practices, some reallocation could still occur. As our data on fishing activity does not cover the time before the introduction of the ban in 1995, we cannot know how fishing activity would evolve over the summer in the absence of the fishing ban. A violation of this assumption would lead to more fishing activity in spring and autumn and hence inflate the estimated reduction in fishing effort due to the ban.

Second, we need to assume that the introduction of the ban in one management zone does not affect fishing activity in another management zone (SUTVA assumption). To test for such spatial spillovers, we replicate our main results from Equation (1) and add a binary variable that is equal to one if a fishing ban is enforced in a neighboring management zone (following the idea in Klauber et al. (2024)). In Table A7 in the Appendix, we show those results and find no significant change in both AIS and VIIRS fishing effort when a fishing ban starts or ends in a neighboring zone. In addition, results from a spatial RDD approach reported in Yuan (2023) also find no increase outside the Chinese EEZ once the fishing ban is in place. This suggests that SUTVA violations may not be a problem on average. However, Figure A3 in the Appendix indicates a potential SUTVA violation in the first management zone: Once the ban has been enforced in zones 3 and 4, AIS fishing effort went up in zone 1. Although an increasing trend of AIS fishing effort started much earlier in management zone 1, we cannot fully rule out concerns about spatial reallocation. A SUTVA violation would lead to more fishing activity in untreated management zones that serve as a control group and hence inflate the reduction in fishing effort due to the ban.

Third, our identification strategy requires a common trend in fishing activity across management zones. This means that fishing activity should have evolved in the same way across management zones if there had been no ban. In Figure A3 in the Appendix, we illustrate the daily fishing activity in each zone by calendar week. Although the long-term trend in fishing activities increases for the first two management zones before the fishing ban, it is stable for the third and fourth management zones. Hence, seasonal patterns might limit support for the common trend assumption. In the short-term, however, we observe relatively stable pre-trends on the days before the ban (see Figure A5 in the Appendix), which can make this assumption more reasonable for event-study designs focussing around the start and end of the ban. We find similar, although noisier, patterns for the VIIRS data.

Fourth, de Chaisemartin and D'Haultfœuille (2020) show that we also need to assume a homogeneous and constant treatment effect over time. This means that the fishing ban should have the same effect in each management zone and that this effect is constant over time. While the fishing ban included more gear types over time and as enforcement efforts also increased (Su et al., 2020), this could suggest an increasing treatment intensity over time. Hence, we will test for heterogeneous treatment effects over time by interacting the treatment variable with annual dummies. Hence, the corresponding regression specifications are:

$$\ln(y^d_{tz}) = \alpha_0 + \sum_{k=2013}^{2019} \beta^k(\text{Ban}_{tz} \times \text{Year}_k) + \gamma_1\text{Moon}_t + \gamma_2\text{Moon}^2_t + \eta\mathbf{X}_{tz} + \mu\mathbf{T}_t + \alpha_{1i} + \epsilon_{tz} \tag{2}$$

Although the treatment effects are relatively stable and similar between years (cf. Figure A6 in the Appendix), the AIS fishing effort appears to slightly increase after 2017, when regulation efforts increased (Su et al., 2020).

Overall, these identification assumptions appear reasonable to a certain degree. However, we cannot fully rule out all, and in particular temporal reallocation and SUTVA. Thus, our estimated reductions in fishing activity should be interpreted with care and may overestimate the reduction in fishing activity due to the ban. In the following time-series model, SUTVA is not required as the model does not exploit variation between management zones. Nonetheless, temporal reallocation can also bias estimates of the time-series model. In addition, the event-study model also requires no temporal reallocation, SUTVA, and a common trend, but is more flexible to capture treatment heterogeneity over time.

Time-series model: In addition to the fixed-effects model, we also apply an OLS time-series model to complement our analysis. While time-series models do not allow us to exploit variation in the timing of the ban between management zones, they can better handle the time-related structure by accounting for serial correlation. Hence, we estimate Equation (1) with an OLS estimator and run additional OLS time-series estimations on sub-samples for each management zone:

$$\ln(y^{dz}_t) = \alpha_0 + \beta\text{Ban}_t + \gamma_1\text{Moon}_t + \gamma_2\text{Moon}^2_t + \eta\mathbf{X}_t + \mu\mathbf{T}_t + \epsilon_t \tag{3}$$

where the unit of observation is simply a given day t and the dependent variable is the sum of total fishing effort as indicated by dataset d in zone z on that day. The coefficient β then measures the average (downward) shift in the fishing effort during the ban period. To identify the ban's effect, the time-series model predicts the counterfactual fishing effort during the ban from the previous and subsequent time-series and compares that to the fitted levels. We visualize this approach in Figure A4 in the Appendix. As serial correlation can be problematic in these OLS time-series estimations, we control for it with Newey-West corrected standard errors. The results are similar between the fixed-effects model and the time-series model, and the time-series model suggests slightly weaker reductions in fishing effort (cf. Table A8). While there is no proper and external control group in the time-series models, however, their results should be interpreted with caution.

Event-study model: Motivated by concerns about constant treatment effects, we also apply an event-study model on our panel dataset following de Chaisemartin and D'Haultfœuille (2023, 2024). Their model allows for heterogeneous treatment effects over time and suits best to our setting for the following reason: Compared to other event-study designs, a particular benefit of their model is that units can enter and leave treatment. In our context, this means that management zones can get treated in spring and exit treatment in autumn again. Other approaches often require an "irreversible treatment" where treated units cannot get untreated again (Callaway and Sant'Anna, 2021). A particularly crucial assumption for this model is, however, the common trend assumption that we discussed before. In addition, the ban's effect is estimated from 20 days around the start and end of the ban period[10] such that the estimates can suffer from less precision in the event-study model compared to the fixed-effects and time-series models.

5 Results

5.1 Reduction in fishing activity due to the ban

We find that the fishing ban significantly reduces fishing activity. In Figure 4, we show the estimated reductions in fishing activity due to the ban using AIS fishing effort and VIIRS boat detections. Overall, we find with our fixed-effects estimation strategy that fishing effort as measured by AIS signals decreases by 90 percent during the ban. As vessels may not be equipped with AIS devices, we then estimate the reduction in fishing activity with VIIRS nighttime lights. By using boat detections from nighttime lights, we confirm a significant reduction in fishing effort during the ban but only estimate a reduction of 48 percent. Our time-series and event-study models suggest similar results: With the time-series model, we estimate a reduction of 85 percent in the AIS fishing effort and of 35 percent in the VIIRS boat detections (see Table A8). In addition, our event-study estimates suggest reductions of 88 percent for AIS fishing effort and 62 percent for VIIRS boat detections (see Figure A5 in the Appendix). While the estimates from the fixed-effects and time-series models are statistically significant at a minimum level of 5 percent, the estimates from the event-study model are less precise due to the few observations around the start and end of the ban period. Reasons for the differences in the estimated reductions relate to the different fishing vessels that are captured by each dataset and by different margins of behavior of those vessels. We will explore those aspects in more detail in the subsequent subsections.

Across management zones, the estimated reductions in fishing activity are similar. For individual management zones, they range between 79 and 94 percent when using AIS data and between 41 and 62 percent when using VIIRS boat detections. Differences between management zones can be related to differences in the local fishing fleets, local enforcement efforts, and local fishing conditions. We will explore some of those differences in the next subsections. Over time, reductions in fishing activity are relatively stable and seem to slightly increase, particularly after 2017, when regulation efforts increased (Su et al., 2020). On average, the reduction in AIS fishing effort due to the ban gets stronger by 0.11 percent per year and the reduction in VIIRS boat detections by 0.03 percent per year (cf. Figure A6 and Table A9 in the Appendix).

[Insert Figure 4 around here]

5.2 Characteristics of non-complying vessels

Our results indicate that vessels using AIS devices seem to reduce their fishing activity more due to the fishing ban than vessels that are detected on nighttime lights. While nighttime lights predominantly capture fishers that target squid and tuna during the night, AIS devices are installed on a variety of fishing vessels regardless of the species they target. This suggests that the level of fishing activity reductions may be related to the targeted species.

When we estimate fishing activity reductions by gear types that have been inferred from AIS signals, we find additional evidence for this conclusion. In Figure A7 in the Appendix, for example, we find the largest reduction in AIS fishing effort during the ban by trawlers and lower reductions by fishers using fixed gear, dredge fishing gear, or other gear types. Considering that the share of trawlers is particularly high in the fourth management zone (cf. Table 1), differences in the local fleet composition also explain differences in the local level of fishing activity reductions shown in Figure 4.

Although we can derive little information on vessels' characteristics from nighttime lights, we can use the brightness of nighttime lights as a proxy for vessels' sizes. Depending on the size of a boat as well as the number and power of their light bulbs, VIIRS boat detections vary in their brightness. As small boats are equipped with only a few light bulbs, large industrial vessels often carry hundreds. We compare the brightness distribution of boats detected by VIIRS nighttime lights during and outside of the ban in Figure A8 in the Appendix. We observe both small-scale fishers with a low radiance and large fishing vessels with a high radiance. Although the brightness levels are lower during the ban, their distribution is similar. Hence, we do not find evidence that boats of a particular size are more prone to noncompliance.

5.3 Location of non-complying vessels

Next, we explore where non-compliance occurs more often. In Figure 5, we map the levels of apparent fishing during the ban. Although fishing is much lower than outside the ban, apparent fishing is widespread and occurs at almost all locations where fishing is also detected outside the ban period. While most AIS signals are captured close to the coast during the ban, many VIIRS boat detections occur particularly in the Gulf of Tonkin at the border to the Vietnamese EEZ and in the second management zone close to the Japanese EEZ. This suggests that some non-compliance might also be caused by foreign vessels that enter the Chinese EEZ during the fishing ban or by Chinese vessels that may evade nautical patrol. Thus, regulators and enforcement agencies may want to focus their monitoring efforts on such areas.

[Insert Figure 5 around here]

In addition, we examine the average fishing activity during the ban depending on the distance to the coast in Figure A9 in the Appendix. If fishers want to avoid the risk of detection, they may avoid coastal waters and move toward more distant waters. However, we do not find evidence of such behavior. Although the reduction in fishing activity is the highest in areas close to the coast, we do not observe higher fishing activity in more distant waters during the ban on average.

5.4 Margins of behavior

Given that some fishing still remains during the fishing ban, a natural question is how fishers evade detection and how they land their catches. We will show that there is more fishing activity detected in the AIS data in evening and nighttime hours during the ban, but that there is also reason to believe that some AIS devices are turned off, suggesting a too-optimistic compliance level. Finally, we show that transshipment events are more likely during the ban which allows fishers to offload catches to refrigerated vessels.

Changes in the time to fish: The fishing ban changes the incentives and costs of fishing. So fishers may hide or target other species, which can lead to changes in the time to fish (Abbott et al., 2015). If fishers using AIS devices start to fish at night, they may increase VIIRS boat detections which would explain part of the heterogeneities in fishing activity reductions.

We explore changes in the daytime to fish in Figure A10 in the Appendix. We find evidence that AIS fishing effort is higher during evening and nighttime hours during the ban. In particular, AIS fishing effort is higher between 5 pm and 6 am during the ban and lower otherwise. Nonetheless, the peak of fishing activity at 6 am and the bottom at around 5 pm are the same during and outside the ban. As the overpass of the VIIRS satellite is fixed between 0.30 and 3.30 am, we are limited to examining changes in the time to fish with the VIIRS nighttime lights.

Offline AIS devices: Fishers engaged in IUU fishing are often difficult to detect with AIS data as they either disable their AIS devices and disappear from the radar or manipulate them and broadcast a wrong location (Park et al., 2023; Taconet et al., 2019). If such practices are common, AIS data would upward bias compliance estimates.

To examine if fishers disable their AIS devices when fishing illegally during the ban, we explore changes in the ratio between AIS vessel hours and AIS fishing hours. AIS vessel hours indicate the time vessels spend outside the harbor with an online AIS device. AIS fishing hours, instead, are only the hours when vessels are actively fishing. If no ban is in place and depending on the management zone, fishers spend on average 41 to 49 percent of their time fishing and are in transit or anchoring for the rest of the time. During the ban, however, the share drops to 33 to 36 percent, which suggests that some fishers may turn off their AIS device when they start fishing during the ban (cf. Table A5 in the Appendix).

We also examine this argument more formally by estimating the reduction in AIS vessel hours due to the ban and compare it with our estimated reductions in AIS fishing effort. If fishers turn off their AIS devices only when they engage in illegal fishing operations during the ban, we would expect a stronger reduction in the AIS fishing effort than in the time they spend making trips (AIS vessel hours). We show our results in Figure A11. We observe that AIS vessel hours show a strong and significant decrease confirming the effectiveness of the ban. However, the reduction in fishing effort is stronger than the reduction in vessel hours, which suggests that some vessels seem to avoid detection by turning off their AIS devices when they appear to fish during the ban.

Landing illicit catches: Given that there is a non-negligible level of fishing effort during the ban, an obvious question is then how fisher land and sell their catch without getting detected.[11] As fishers can continue fishing outside the Chinese EEZ, landing and processing sites must not close down during the fishing ban. In addition, fishers can also land their catch at private sites, at foreign ports, or transship them to other vessels. Transshipment is a practice done on high seas where a fishing vessel offloads its catch to a refrigerated cargo vessel (Miller et al., 2018). This can hide the actual source of catch and make enforcement difficult. In Figure A12 in the Appendix, we explore the location of potential transshipment events and compare the number of potential transshipment events on days with and without the fishing ban in Figure A13 in the Appendix. Although there are only a few instances where a fishing vessel encountered a cargo vessel long enough to offload catch, we observe many instances where a cargo vessel loitered long enough to receive catch and consider those as potential transshipment events (Miller et al., 2018). We find that the daily number of potential transshipment events is significantly higher on average in the first three management zones during the fishing ban, which suggests that transshipment seems a frequent activity for non-complying fishing vessels to avoid detection.

5.5 Income opportunities and non-compliance

Finally, we explore the role of income opportunities to understand the reasons for non-compliance. Given that the fishing ban eliminates income opportunities from fishing, affected households could diversify their income sources and generate income from other sources. The average Chinese fisher is, however, very dependent on fishing income. In 2020, the average household income of Chinese fishers was $72,538$ Yuan (approx. $10,513$ USD) per person, and more than 84 percent of it came from fishery-related activities as we show in Table A2 in the Appendix (China Fishery Statistical Yearbook, 2020). Similarly, social transfers and fishing subsidies which could compensate for the loss of income during the ban only contribute to less than 4 percent of households' total income.[12] At the same time, opportunities for switching to other jobs and businesses during the ban are often limited for many small-scale fishers due to their low average education, inadequate access to financial markets, and as fishing often represents a cultural activity done for generations (Zhao and Jia, 2020). Thus, the need to maintain subsistence based on marine fishing may lead to non-compliance with the fishing ban for some fishers.

Besides income opportunities in other industries, income opportunities in fisheries may trigger non-compliance with the ban. To this end, we explore the relationship between non-compliance and income opportunities similar to Axbard (2016) and Flückiger and Ludwig (2015). They find that fishing conditions are negatively associated with the number of piracy attacks and suggest that fishers are more likely to engage in sea piracy when income opportunities in their fisheries are low. In a similar vein, we expect that apparent fishing during the ban is also more likely when income opportunities are excellent. Because when fishing is prohibited and fishing conditions are excellent, the opportunity costs of compliance might be too high.

Previous studies find that phytoplankton abundance can explain fishing conditions. Axbard (2016) shows, for example, that phytoplankton abundance reduces prices and affects labor market outcomes such as income and time spent on fishery-related activities in Indonesia. In addition, Flückiger and Ludwig (2015) show that phytoplankton abundance increases fish capture production even for a larger sample of 109 coastal countries. As we do not have information on fish prices, catch records, or labor market outcomes, we assume this result also holds in our context. Similar to Flückiger and Ludwig (2015), we use the phytoplankton absorption coefficient at 443 nm from NASA's Moderate Resolution Imaging Spectroradiometer (MODIS) Aqua satellite as a proxy for the phytoplankton abundance and map it for 2019 in Figure A14 in the Appendix.

To explore the link between fishing conditions and non-compliance, we estimate a fixed-effects regression. In particular, we use our grid sample and estimate the probability of detecting local fishing activity as well as the level of fishing activity, depending on fishing conditions. While phytoplankton depends, among others, on sea-surface temperature, we treat its temporal and spatial variation as exogenous. Thus, we estimate the following fixed-effects specification:

$$y^d_{wc} = \beta_1 \text{Aph}_{wc} + \beta_2 \text{Ban}_{wc} + \beta_3 \left(\text{Aph}_{wc} \times \text{Ban}_{wc}\right) + \eta_w + \alpha_c + \epsilon_{wc} \tag{4}$$

where y^d_{wc} indicates the occurrence or level of fishing activity y in week w in grid cell c as indicated by data d (either AIS fishing effort or VIIRS boat detections). Aph_{wc} captures the phytoplankton abundance and serves as a proxy for good fishing conditions. Ban_{wc} is a binary dummy variable equal to one if the fishing ban is in place in grid cell c in week w. η_w controls for time fixed effects, α_c for grid cell fixed effects and ϵ_{wc} captures any remaining residuals. Our coefficient of interest is β_3 for the interaction term between phytoplankton abundance and the fishing ban. This coefficient indicates how apparent fishing activity reacts to changes in the fishing conditions during the ban. We use the same correction of standard errors following Conley (1999, 2008) for this estimation as described in Section 4.

Table 2 shows our results. Overall, we find that phytoplankton abundance affects fishing activity. We find an increase in the probability to detect of fishing activity in the VIIRS data (Column 2), which is consistent with previous findings (Axbard, 2016; Flückiger and Ludwig, 2015). There seems, however, less AIS fishing effort when phytoplankton is high (Column 1). This is surprising as we would expect both measures of fishing activity to increase. Similar to previously documented practices, we suspect that fishers also disable AIS devices in areas with lots of phytoplankton to avoid competition – a practice that has previously documented by Welch et al. (2022). The key variable of interest in this analysis is then the interaction between phytoplankton abundance and the fishing ban. In Columns (1) and (2), we find that an increase in the phytoplankton abundance by one standard deviation during the fishing ban increases the probability of detecting fishing activity by 3.2 [5.2] percent in the AIS [VIIRS] data. In addition, an increase in the phytoplankton abundance during the fishing ban also increases the level of local fishing activity, as we show in Columns (3) and (4).[13] In line with previous studies, we therefore conclude that the lack of income opportunities in other industries, and excellent income opportunities in fisheries hamper compliance with fishing regulations and increase apparent fishing during the ban.

[Insert Table 2 around here]

6 Robustness Checks

To substantiate our results, we provide additional robustness checks on the estimated reductions in AIS fishing effort and VIIRS boat detections.

Fishing detections from synthetic-aperture radar (SAR): Besides the AIS and VIIRS data, we also explore another dataset with fishing detections from synthetic-aperture radar (SAR) images of the Sentinel-1 satellites (Paolo et al., 2024). Compared to the AIS data, vessels must not be equipped with any tracking device to be detected. And compared to VIIRS nighttime lights, SAR images are taken at around 6 am or 6 pm local time and are unaffected by clouds and the moon phase. Hence, they capture a broader set of vessels than the VIIRS data.

Paolo et al. (2024) provide a processed time series of fishing detections at the EEZ level which we use to estimate the reduction in fishing activity due to the ban. As the data is a simple time series without a panel structure, we apply our time-series model following Equation (3). As the dependent variable, we use the daily total number of SAR fishing detections in the Chinese EEZ. A notable difference to our main estimation is, however, the ban dummy. As we run the estimation on the EEZ level, the independent variable ban ranges between zero and one and denotes the share of management zones that have the fishing ban in place. For example, the variable is equal to zero if the ban is not in place anywhere, equal to 0.5 if two out of the four management zones have the ban in place, and equal to one if all management zones have the fishing ban in place.

With the SAR data, we find a reduction in fishing activity due to the ban by 74 percent (see Table A10 in the Appendix). This is in between the estimated reduction of 85 percent with the AIS data and the 35 percent reduction by the VIIRS data when using the same time-series model (cf. Table A8 Column (2) in the Appendix). For vessels that are detected by SAR and that could be matched to AIS signals, the reduction is 84 percent. For so-called "dark vessel" that could not be matched with AIS signals, the reduction is 65 percent. This confirms that the fishing ban is effective in reducing fishing activity. Again, vessels that broadcast AIS signals seem to reduce their fishing activity stronger than others. However, among those fishing vessels that do not use AIS devices, the reduction in fishing activity seems stronger than that suggested by the VIIRS boat detections during the night. This suggests that vessels that fish with light during the night may react the weakest to the fishing regulation.

Different sample and regression specifications: Next, we re-estimate the effect of the fishing ban on fishing activity using the grid sample in addition to the zone sample. Due to the limited number of VIIRS boat detections in a given week and cell, we will use a binary dummy that is equal to one if fishing activity is detected in a given week and cell as the outcome variable and not the level of fishing activity. Compared to our main results, we can interpret coefficients as the changes in the probability that fishing activity occurs.[14]. In Table A11 in the Appendix, we show those results which confirm our main results. We find that the likelihood that AIS fishing activity is detected in a given grid cell and week decreases by 0.12 percent on average due to the ban and by 0.07 percent for VIIRS boat detections. Hence, vessels using AIS devices seem to respond stronger than vessels using nighttime light.

In addition, we explore how results change for different regression specifications. To this end, we also add month-fixed effects to our base specification in Equation 1 and find similar results in Table A12 in the Appendix. As the fishing ban is everywhere in force in certain months (cf. Table A1), these month-fixed effects capture some of the reduction in fishing activity which should be attributed to the fishing ban. Nonetheless, they confirm our main results. Moreover, clustering standard errors on both the yearly and monthly levels suggests similar results.

Measurement error: Finally, we explore how measurement error could affect our estimates. One source of measurement error is the data generation process of the fishing effort. While both AIS fishing effort and VIIRS boat detections are measures of predicted fishing efforts based on machine learning, imprecise classifications could bias our results. We address this concern by providing insights on the size of measurement error that we expect from the machine learning algorithms similar to Park et al. (2020).

There are two ways in which these algorithms can contribute to measurement error. If fishing activity or fishing boats are not detected (false-negatives), we would overestimate reductions in fishing activity. On the other hand, if fishing activity or fishing boats are incorrectly classified as such (false positives), we would underestimate reductions in fishing activity. We assume that there is no interaction between measurement error in both datasets so that it affects reductions in fishing activity independently of each other. We are not aware of any other seasonal patterns that could affect measurement error during the fishing ban and assume it is constant. Kroodsma et al. (2018) reports an overall accuracy of 90 percent, and reports higher accuracy rates between 91 and 97 percent for specific gear types. We assume that measurement error is equally likely for all vessels and use the conservative accuracy rate of 90 percent for our robustness check. This means that more than 90 percent of the predictions are correct and that the sum of false-positives and false-negatives cannot exceed 10 percent. Hence, the actual level of AIS fishing effort could be 10 percent higher or lower.

To understand how measurement error would affect our results, we re-run our main estimation where we either (i) add 10 percent of the fishing effort (i.e., the one which might not have been detected) or (ii) remove 10 percent of the fishing effort (i.e., the one which might have been falsely classified as such). For the VIIRS boat detection algorithm, Elvidge et al. (2018) show in a validation exercise that 4 out of 594 boats have not been detected by the VIIRS boat detection algorithm, which suggests a false-negative rate of 0.7 percent. While they do not provide insights on the rate of false-positives, Park et al. (2020) reconstruct them and suggest a rate of false positives of around 1 to 2 detections per million square kilometers per day, which is almost the size of the Chinese EEZ. In a similar vein, we also re-run our main estimation with the VIIRS boat detections and either (i) add 2 boat detections each day (i.e., those which might not have been detected) or (ii) remove 0.7 percent of the boat detections (i.e., those which might have been falsely classified as such). This acknowledges that the actual number of boats that should be classified correctly could be higher or lower.

We show our results in Figure A15 in the Appendix. While measurement error could change the estimated average reduction in AIS fishing effort to a range of 87.2 to 91.9 percent, it has almost no impact on the estimated fishing activity reductions using VIIRS boat detections. As the accuracy of the AIS fishing detection algorithm varies across fishing gears, we also re-run our main estimation for some gear types separately. We report those results in Figure A16 in the Appendix and find consistent results with only small changes to the estimated fishing activity reductions of specific gear types.

Finally, another source of measurement error is relevant for the AIS data as AIS satellites can only capture a maximum number of signals at a time. This can lead to a lower level of AIS fishing effort and measurement error could bias our results. While AIS reception quality improved significantly from 2016 (Taconet et al., 2019), we re-run our main estimations for data from 2016. We find consistent results with our main results, which we present in Figure A17 in the Appendix.

7 Conclusion

This paper evaluates reductions in fishing activity due to the annual Chinese fishing ban. Besides revealing intended reductions in fishing activity, we also explore unintended adaptive behaviors. We use two different measures of fishing activity to estimate the reduction in fishing activity due to the ban. Besides data from vessel broadcast positions (AIS), we use data from nighttime lights (VIIRS). The former data captures more vessels and fishing gear but requires boats to be equipped with AIS devices. The latter data, in contrast, largely captures fishers targeting squid and tuna who are using lights at night to attract fish. Together both measures complement each other and allow for comprehensive insights into the activities of fishing vessels during the fishing ban. For the overall Chinese EEZ, our results suggest a significant and substantial reduction in fishing activity due to the ban. While data on vessel broadcast positions suggest an average reduction in fishing activity of 90 percent, we find a reduction of half that size when relying on nighttime lights. We then explore the characteristics and locations of non-complying vessels.

We find that vessels fish more during evening and nighttime hours, that fishers disable vessel broadcast position devices, and that they seem to offload catch to refrigerated cargo vessels more often during the ban. Finally, the lack of outside options and excellent fishing conditions during the ban hamper compliance.

One limitation of our study relates to the data. Both measures of fishing activity are predicted measures. Although there are limitations in detecting fishing activity from AIS signals and nighttime lights, this data provides a valuable, independent, and global measure of fishing activity, which allows for similar policy evaluations in other contexts. Similarly, our measures of fishing activity are uninformative about vessel's productivity or their harvest. As a result, we are limited in assessing the ban's impact on fish stocks and the health of the ecosystem.

In addition, our empirical estimates rest on a few assumptions which are partly shared by our different identification strategies. Although these assumptions appear reasonable on average, we cannot fully rule out concerns regarding temporal reallocation and SUTVA. We show that violations can overestimate the estimated treatment effect of the ban and note that the estimated reductions in fishing activity due to the ban should be interpreted with care.

Another limitation is related to the definition of the Chinese EEZ border. While we rely on the official border of the Chinese EEZ (as described by Flanders Marine Institute, 2014), there are ongoing disputes and claims from China to neighboring areas. As there are some reports that China is enforcing its ban also in disputed areas (cf. Inquirer, 2020), our estimates are rather conservative and do not include fishing activity in disputed areas. We, thus, leave it open for future research to investigate potential spillovers in neighboring areas. Finally, our estimated reductions in fishing activity only relate to the Chinese annual fishing ban. We cannot detect IUU fishing in general, nor can we estimate how IUU fishing changes with the fishing ban.

Overall, our results offer important insights for marine regulators, international fishery organizations, and enforcement agencies. Although we find a substantial level of fishing activity reductions on average, targeted enforcement towards specific vessels, gear types, and locations could be promising. We also document several facts and practices on how non-complying fishers respond to the policy, which helps in designing better policies to ultimately improve resource conservation. And finally, we show that remotely sensed data can complement traditional vessel monitoring systems to monitor regulation and reduce the costs of regulation.

Acknowledgments

For comments and helpful suggestions on earlier drafts, I thank Josh Abbott, Pier Basaglia, Florian Diekert, Moritz Drupp, Gabe Englander, Tillmann Eymess, Andreas Lange, Grischa Perino, Luciana Puebla, Martin Quaas, Marie Riekhoff, Swantje Sundt, Michael Tanner, Haishan Yuan, and many seminar and conference participants at the University of Hamburg, University of Kiel, University of Leipzig, University of California Santa Barbara, at the NAAFE webinar series, and the EAERE conference 2021. Financial support by the German Ministry of Education and Research (grant 01LC1826B, *marEEshift*) is greatly appreciated.

Footnotes

[1]We define "overfished" as the biomass that is less than 80% of the catch-maximizing biomass and "too high fishing pressure" as that above the catch-maximizing fishing pressure.

[2]We are cautious with calling this fishing activity *illegal*. While the measures of fishing effort are statistical estimates of machine learning algorithms and of data that was not designed to measure fishing effort in the first place, some fishing activity might not be captured or misclassified. Therefore, we follow Global Fishing Watch's definition and refer to *apparent* fishing effort to reflect this underlying certainty.

[3]We end our study period before the COVID-19 pandemic since regional (fishing) restrictions to contain the pandemic had major impacts on fishing operations (Paolo et al., 2024)

[4]We illustrate a positive and significant correlation between both datasets in Figure A2 and Table A3 in the Appendix. However, there are only a few squid and tuna fishers reliably identified as such in our study from the AIS data which restricts the overlap for our study.

[5]Besides fishing, there are also other economic activities on sea, like the extraction of oil and gas, offshore drilling, or sea traffic that might be captured with the satellite observations during the night. To rule them out, we exclude detections of stationary nighttime lights that reoccur at the same location, detections at known locations of gas flares, and those that coincide with infrared radiant emissions from combustion sources. We also exclude boat detections that have been classified as blurry. To exclude sea traffic, the boat detection algorithm has been developed to filter for those light sources that nighttime fishers use. A validation of the boat detection algorithm with the Indonesian VMS concludes that boats that do not use light to attract catch "are only occasionally detected when nighttime operations call for extra deck lightning" (Hsu et al., 2019).

[6]We acknowledge that fishers could theoretically avoid detection by turning off their light during the overpass of the satellite. However, we are not aware of any reports that confirm such a practice.

[7]Note that the difference in the average fishing activities does not represent the policy effect as it does not consider the counterfactual fishing level that would take place in the absence of the ban. Besides the significant difference in the mean VIIRS boat detections, Yuan (2023) detects significant regression discontinuities around the start and end of the ban, which shows that VIIRS boat detections pick up the

fishing ban and do not follow a random walk.

[8]Technically, we would measure the intensive margin with the AIS data (i.e., the reduction in fishing effort given that some fishing occurs on a given day) and the extensive margin with the VIIRS data (i.e., the reduction of active fishing vessels independent of fishing activity at a given day). As there are, however, no days without any fishing activity, results from both measures can be interpreted as the intensive margin.

[9]In a related paper, using VIIRS data only, Yuan (2023) estimates a slightly larger change in fishing activity after the lift of the ban than at the beginning. They also show that preemptive and reactive compliance efforts seem limited as boat detections start to decrease only 2 nights before the start of the ban, which can be the time to return to a harbor, and that boat detections do not seem to increase before the lift of the ban.

[10]The length of the event window is restricted methodologically. The 10 days before and after are chosen to balance precision and power while still retaining an appropriate counterfactual pre-event fishing activity level.

[11]Similarly, for coastal communities and supply chains, it is also important to understand *where* fish is landed (cf. Cojocaru et al., 2019), but we leave this open fur future research due to data limitations.

[12]Remittances by family members employed in other industries may also supplement fishers' household income, but we are not aware of their importance in our study context. In fact, education and family size are often key determinants for remittances and off-resource labor supply but can affect both in different directions which makes it difficult to form expectations in our context (Eskander et al., 2018).

[13]We cannot compare the coefficients in Columns (3) and (4) with each other as the underlying grid cells and the number of observations are different. As we observe fewer grid cell-week observations with AIS fishing effort than with VIIRS boat detections.

[14]Please note that this estimation resembles a fuzzy differences-in-differences setting as the ban can could be both in and out of force in a given week (de Chaisemartin and D'Haultfœuille, 2018). Likewise, for grid cells with intersections of two management zones, the ban could also be in force in some parts, while it could be out of force in other areas. If the ban is in place on any day during a week or in any area of a cell, we assume it receives treatment. Hence, the grid sample likely underestimates reductions in fishing activity

References

Abbott, J. K., A. C. Haynie, and M. N. Reimer (2015). Hidden flexibility: Institutions, incentives, and the margins of selectivity in fishing. *Land Economics 91*(1), 169–195.

Agnew, D. J., J. Pearce, G. Pramod, T. Peatman, R. Watson, J. R. Beddington, and T. J. Pitcher (2009). Estimating the Worldwide Extent of Illegal Fishing. *PLOS ONE 4*(2), e4570.

Axbard, S. (2016). Income Opportunities and Sea Piracy in Indonesia: Evidence from Satellite Data. *American Economic Journal: Applied Economics 8*(2), 154–194.

Burke, M., A. Driscoll, D. Lobell, and S. Ermon (2020). Using Satellite Imagery to Understand

and Promote Sustainable Development. Working Paper w27879, National Bureau of Economic Research, Cambridge, MA.

Cabral, R. B., J. Mayorga, M. Clemence, J. Lynham, S. Koeshendrajana, U. Muawanah, D. Nugroho, Z. Anna, Mira, A. Ghofar, N. Zulbainarni, S. D. Gaines, and C. Costello (2018). Rapid and lasting gains from solving illegal fishing. *Nature Ecology & Evolution 2*(4), 650–658.

Callaway, B. and P. H. Sant'Anna (2021). Difference-in-Differences with multiple time periods. *Journal of Econometrics 225*(2), 200–230.

Cameron, A. C., J. B. Gelbach, and D. L. Miller (2008). Bootstrap-Based Improvements for Inference with Clustered Errors. *Review of Economics and Statistics*.

Cao, L., Y. Chen, S. Dong, A. Hanson, B. Huang, D. Leadbitter, D. C. Little, E. K. Pikitch, Y. Qiu, Y. Sadovy de Mitcheson, U. R. Sumaila, M. Williams, G. Xue, Y. Ye, W. Zhang, Y. Zhou, P. Zhuang, and R. L. Naylor (2017). Opportunity for marine fisheries reform in China. *Proceedings of the National Academy of Sciences 114*(3), 435–442.

China Fishery Statistical Yearbook (2020). Ministry of Agriculture and Rural Affairs of the People's Republic of China Bureau of Fisheries. China Agriculture Press.

Cojocaru, A. L., F. Asche, R. B. M. Pincinato, and H.-M. Straume (2019). Where Are the Fish Landed? An Analysis of Landing Plants in Norway. *Land Economics 95*(2), 246–257.

Conley, T. (1999). GMM estimation with cross sectional dependence. *Journal of Econometrics 92*(1), 1–45.

Conley, T. G. (2008). Spatial Econometrics. In Palgrave Macmillan (Ed.), *The New Palgrave Dictionary of Economics*, pp. 1–9. London: Palgrave Macmillan UK.

Costello, C., D. Ovando, T. Clavelle, C. K. Strauss, R. Hilborn, M. C. Melnychuk, T. A. Branch, S. D. Gaines, C. S. Szuwalski, R. B. Cabral, D. N. Rader, and A. Leland (2016). Global fishery prospects under contrasting management regimes. *Proceedings of the National Academy of Sciences 113*(18), 5125–5129.

de Chaisemartin, C. and X. D'Haultfœuille (2018). Fuzzy Differences-in-Differences. *The Review of Economic Studies 85*(2), 999–1028.

de Chaisemartin, C. and X. D'Haultfœuille (2020). Two-Way Fixed Effects Estimators with Heterogeneous Treatment Effects. *American Economic Review 110*(9), 2964–2996.

de Chaisemartin, C. and X. D'Haultfœuille (2023). Two-way fixed effects and differences-in-differences estimators with several treatments. *Journal of Econometrics 236*(2), 105480.

de Chaisemartin, C. and X. D'Haultfœuille (2024). Difference-in-Differences Estimators of Intertemporal Treatment Effects. *Review of Economics and Statistics*. Forthcoming.

De Souza, E. N., K. Boerder, S. Matwin, and B. Worm (2016). Improving Fishing Pattern Detection from Satellite AIS Using Data Mining and Machine Learning. *PLOS ONE 11*(9), e0163760.

Diekert, F., L. Nøstbakken, and A. Richter (2021). Control activities and compliance behavior—Survey evidence from Norway. *Marine Policy 125*, 104381.

Donaldson, D. and A. Storeygard (2016). The View from Above: Applications of Satellite Data in Economics. *Journal of Economic Perspectives 30*(4), 171–198.

Drupp, M. A., M. Khadjavi, and M. F. Quaas (2019). Truth-telling and the regulator. Experimental evidence from commercial fishermen. *European Economic Review 120*, 103310.

Elvidge, C. D., K. Baugh, M. Zhizhin, F.-C. Hsu, and T. Ghosh (2017). VIIRS night-time lights. *International Journal of Remote Sensing 38*(21), 5860–5879.

Elvidge, C. D., T. Ghosh, K. Baugh, M. Zhizhin, F.-C. Hsu, N. S. Katada, W. Penalosa, and B. Q. Hung (2018). Rating the Effectiveness of Fishery Closures With Visible Infrared Imaging Radiometer Suite Boat Detection Data. *Frontiers in Marine Science 5*, 132.

Elvidge, C. D., M. Zhizhin, K. Baugh, and F.-C. Hsu (2015). Automatic Boat Identification System for VIIRS Low Light Imaging Data. *Remote Sensing 7*(3), 3020–3036.

Englander, G. (2019). Property rights and the protection of global marine resources. *Nature Sustainability 2*(10), 981–987.

Eskander, S. M., E. B. Barbier, and B. Gilbert (2018). Fishing and Nonfishing Income Decisions: The Role of Human Capital and Family Structure. *Land Economics 94*(1), 114–136.

FAO (2018). *The State of World Fisheries and Aquaculture 2018 - Meeting the Sustainable Development Goals.* Rome, Italy.

FAO (2024). Fishery Statistics – Global Capture Production. URL: `https://www.fao.org/fishery/en/collection/capture?lang=en`. Last accessed on June 26, 2024.

Flanders Marine Institute (2014). Maritime Boundaries Geodatabase, Version 10. URL: `https://www.marineregions.org/downloads.php`. Last accessed on January 12, 2021.

Flückiger, M. and M. Ludwig (2015). Economic shocks in the fisheries sector and maritime piracy. *Journal of Development Economics 114*, 107–125.

Gonzalez-Lira, A. and A. M. Mobarak (2021). Slippery Fish: Enforcing Regulation when Agents Learn and Adapt. Technical Report w28610, National Bureau of Economic Research, Cambridge, MA.

Goodman-Bacon, A. (2021). Difference-in-Differences with Variation in Treatment Timing. *Journal of Econometrics*, 49.

Grainger, C. A. and D. P. Parker (2013). The Political Economy of Fishery Reform. *Annual Review of Resource Economics 5*(1), 369–386.

Henderson, J. V., A. Storeygard, and D. N. Weil (2012). Measuring Economic Growth from Outer Space. *American Economic Review 102*(2), 994–1028.

Hilborn, R., R. O. Amoroso, C. M. Anderson, J. K. Baum, T. A. Branch, C. Costello, C. L. de Moor, A. Faraj, D. Hively, O. P. Jensen, H. Kurota, L. R. Little, P. Mace, T. McClanahan, M. C. Melnychuk, C. Minto, G. C. Osio, A. M. Parma, M. Pons, S. Segurado, C. S. Szuwalski, J. R. Wilson, and Y. Ye (2020). Effective fisheries management instrumental in improving fish stock status. *Proceedings of the National Academy of Sciences 117*(4), 2218–2224.

Hsu, F.-C., C. D. Elvidge, K. Baugh, M. Zhizhin, T. Ghosh, D. Kroodsma, A. Susanto, W. Budy, M. Riyanto, R. Nurzeha, and Y. Sudarja (2019). Cross-Matching VIIRS Boat Detections with Vessel Monitoring System Tracks in Indonesia. *Remote Sensing 11*(9), 995.

Inquirer (2020). PH Protests China's Fishing Ban; Says Beijing Can't 'Legally Enforce' It in West PH Sea Read. `https://globalnation.inquirer.net/196332/ph-protests-chinas-fishing-ban-says-beijing-cant-legally-enforce-it-in-west-ph-sea`. Last accessed on June 10, 2021.

Jain, M. (2020). The Benefits and Pitfalls of Using Satellite Data for Causal Inference. *Review of Environmental Economics and Policy 14*(1), 157–169.

Klauber, H., F. Holub, N. Koch, N. Pestel, N. Ritter, and A. Rohlf (2024). Killing Prescriptions Softly: Low Emission Zones and Child Health from Birth to School. *American Economic Journal: Economic Policy*. forthcoming.

Kroodsma, D. A., J. Mayorga, T. Hochberg, N. A. Miller, K. Boerder, F. Ferretti, A. Wilson, B. Bergman, T. D. White, B. A. Block, P. Woods, B. Sullivan, C. Costello, and B. Worm (2018). Tracking the global footprint of fisheries. *Science 359*(6378), 904–908.

Lu, Y., Y. Zhang, X. Cao, C. Wang, Y. Wang, M. Zhang, R. C. Ferrier, A. Jenkins, J. Yuan, M. J. Bailey, D. Chen, H. Tian, H. Li, E. U. von Weizsäcker, and Z. Zhang (2019). Forty years of reform and opening up: China's progress toward a sustainable path. *Science Advances 5*(8), eaau9413.

McCauley, D. J., P. Woods, B. Sullivan, B. Bergman, C. Jablonicky, A. Roan, M. Hirshfield, K. Boerder, and B. Worm (2016). Ending hide and seek at sea. *Science 351*(6278), 1148–1150.

McDonald, G. G., C. Costello, J. Bone, R. B. Cabral, V. Farabee, T. Hochberg, D. Kroodsma, T. Mangin, K. C. Meng, and O. Zahn (2021). Satellites can reveal global extent of forced labor in the world's fishing fleet. *Proceedings of the National Academy of Sciences 118*(3), e2016238117.

Miller, N. A., A. Roan, T. Hochberg, J. Amos, and D. A. Kroodsma (2018). Identifying Global Patterns of Transshipment Behavior. *Frontiers in Marine Science 5*, 240.

Ministry of Agriculture (2012). Interim Measures for the Monitoring and Management of the Position of Offshore Fishing Vessels.

Ministry of Agriculture (2013). Guiding Opinions on the Implementation of Agricultural Machinery Purchase Subsidies in 2013.

Ministry of Agriculture (2020). The ten typical cases of violations of laws and regulations related to fishing in 2019. `http://www.gov.cn/xinwen/2020-04/28/content_5506968.htm`. Last accessed on March 7, 2023.

NASA Goddard Space Flight Center, Ocean Ecology Laboratory, and Ocean Biology Processing Group (2018). Moderate-resolution Imaging Spectroradiometer (MODIS) Aqua Ocean Color Data. Last accessed on August 25, 2021.

Nøstbakken, L. (2008). Fisheries law enforcement—A survey of the economic literature. *Marine Policy 32*(3), 293–300.

OECD (2020). *OECD Review of Fisheries 2020*. OECD Review of Fisheries: Policies and Summary Statistics. Paris: OECD Publishing.

Oozeki, Y., D. Inagake, T. Saito, M. Okazaki, I. Fusejima, M. Hotai, T. Watanabe, H. Sugisaki, and M. Miyahara (2018). Reliable estimation of IUU fishing catch amounts in the northwestern Pacific adjacent to the Japanese EEZ: Potential for usage of satellite remote sensing images. *Marine Policy 88*, 64–74.

Paolo, F., D. Kroodsma, J. Raynor, T. Hochberg, P. Davis, J. Cleary, L. Marsaglia, S. Orofino, C. Thomas, and P. Halpin (2024). Satellite mapping reveals extensive industrial activity at sea. *Nature 625*(7993), 85–91.

Park, J., J. Lee, K. Seto, T. Hochberg, B. A. Wong, N. A. Miller, K. Takasaki, H. Kubota, Y. Oozeki, S. Doshi, M. Midzik, Q. Hanich, B. Sullivan, P. Woods, and D. A. Kroodsma (2020). Illuminating dark fishing fleets in North Korea. *Science Advances 6*(30), eabb1197.

Park, J., J. Van Osdel, J. Turner, C. M. Farthing, N. A. Miller, H. L. Linder, G. Ortuño Crespo, G. Carmine, and D. A. Kroodsma (2023). Tracking elusive and shifting identities of the global fishing fleet. *Science Advances 9*(3), eabp8200.

Riekhof, M.-C. and F. Noack (2022). Nature's decline and recovery – Structural change, regulatory costs, and the onset of resource use regulation. Available at `https://papers.ssrn.com/sol3/papers.cfm?abstract_id=4246581`.

Seto, K. L., N. A. Miller, D. Kroodsma, Q. Hanich, M. Miyahara, R. Saito, K. Boerder, M. Tsuda, Y. Oozeki, and O. Urrutia S. (2023). Fishing through the cracks: The unregulated nature of global squid fisheries. *Science Advances 9*(10), eadd8125.

Shen, G. and M. Heino (2014). An overview of marine fisheries management in China. *Marine Policy 44*, 265–272.

Spijkers, J., G. Singh, R. Blasiak, T. H. Morrison, P. Le Billon, and H. Österblom (2019). Global patterns of fisheries conflict: Forty years of data. *Global Environmental Change 57*, 101921.

Stavins, R. N. (2011). The Problem of the Commons: Still Unsettled after 100 Years. *American Economic Review 101*(1), 81–108.

Su, S., Y. Tang, B. Chang, W. Zhu, and Y. Chen (2020). Evolution of marine fisheries management in China from 1949 to 2019: How did China get here and where does China go next? *Fish and Fisheries 21*(2), 435–452.

Sumaila, U. R., D. Zeller, L. Hood, M. L. D. Palomares, Y. Li, and D. Pauly (2020). Illicit trade in marine fish catch and its effects on ecosystems and people worldwide. *Science Advances 6*(9), eaaz3801.

Taconet, M., D. Kroodsma, and J. A. Fernandes (2019). *Global Atlas of AIS-based Fishing Activity: Challenges and Opportunities*. Rome: FAO.

Tickler, D., J. J. Meeuwig, K. Bryant, F. David, J. A. H. Forrest, E. Gordon, J. J. Larsen, B. Oh, D. Pauly, U. R. Sumaila, and D. Zeller (2018). Modern slavery and the race to fish. *Nature Communications 9*(4643).

UN (1982). United Nations Convention on the Law of the Sea. Technical report.

UN (2015). *Transforming Our World: The 2030 Agenda for Sustainable Development*. New York, USA.

Vollaard, B. and S. Kastoryano (2023). Unseen annihilation: Illegal fishing practices and nautical patrol. *Journal of Environmental Economics and Management 122*, 102881.

Watson, R. and D. Pauly (2001). Systematic distortions in world fisheries catch trends. *Nature 414*(6863), 534–536.

Welch, H., T. Clavelle, T. D. White, M. A. Cimino, J. Van Osdel, T. Hochberg, D. Kroodsma, and E. L. Hazen (2022). Hot spots of unseen fishing vessels. *Science Advances 8*(44), eabq2109.

Yuan, H. (2023). Fishing Ban. URL: `https://haishan-yuan.github.io/docs/FishingBan2023Oct.pdf`. Unpublished Manuscript.

Zhao, X. and P. Jia (2020). Towards sustainable small-scale fisheries in china: A case study of hainan. *Marine Policy 121*.

Main Figures and Tables

Figure 1: Fishing activity in our study region

(a) AIS fishing effort (b) VIIRS boat detections

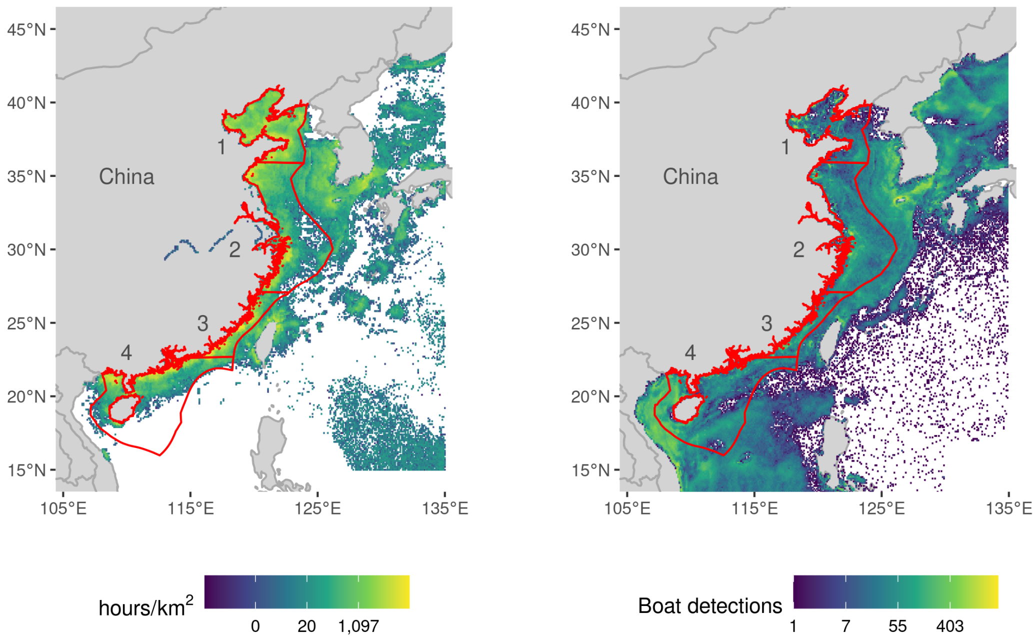

Notes: Both maps show the overall fishing activity in the Chinese EEZ and neighboring regions in 2019 from different data sources. Subfigure (A) depicts the fishing effort measured in hours per square kilometer using vessel broadcast information from the AIS system (Kroodsma et al., 2018). Subfigure (B) depicts the number of boat detections derived from nighttime lights (Elvidge et al., 2015). The red areas and gray numbers indicate the respective management zones within the Chinese EEZ.

Figure 2: Nighttime lights and boat detections at the Gulf of Tonkin

(a) VIIRS image

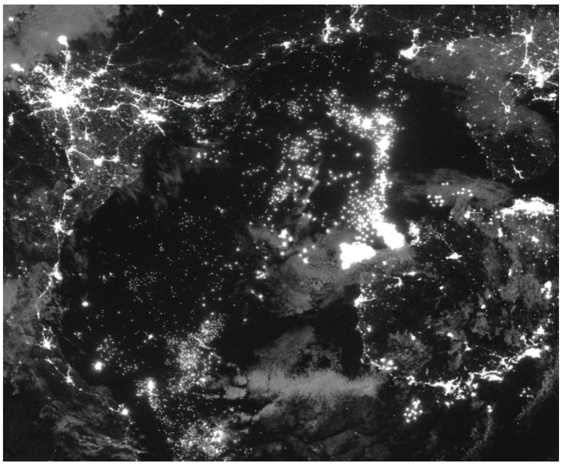

(b) VIIRS boat detections

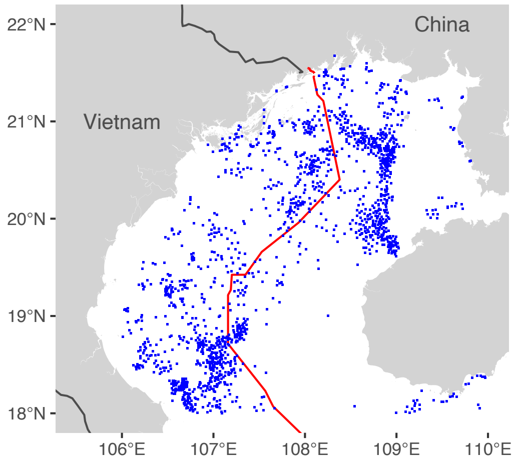

Notes: The figure shows an example VIIRS satellite image and the corresponding fishing boat detections. Subfigure (a) shows an example image taken by the VIIRS satellite on February 17, 2017, at the Gulf of Tonkin. Subfigure (B) shows the result of the VIIRS boat detection algorithm (Elvidge et al., 2015). Blue dots indicate the location of boat detections, the black line indicates the coastlines of China and Vietnam, and the red line the border of the Chinese EEZ. A boat detection indicates fishing activity in an area of 742m $\times$ 742m at the overpass of the VIIRS satellite between around 00:30 and 03:30 each night.

Figure 3: Fishing activity over time in the North Yellow Sea

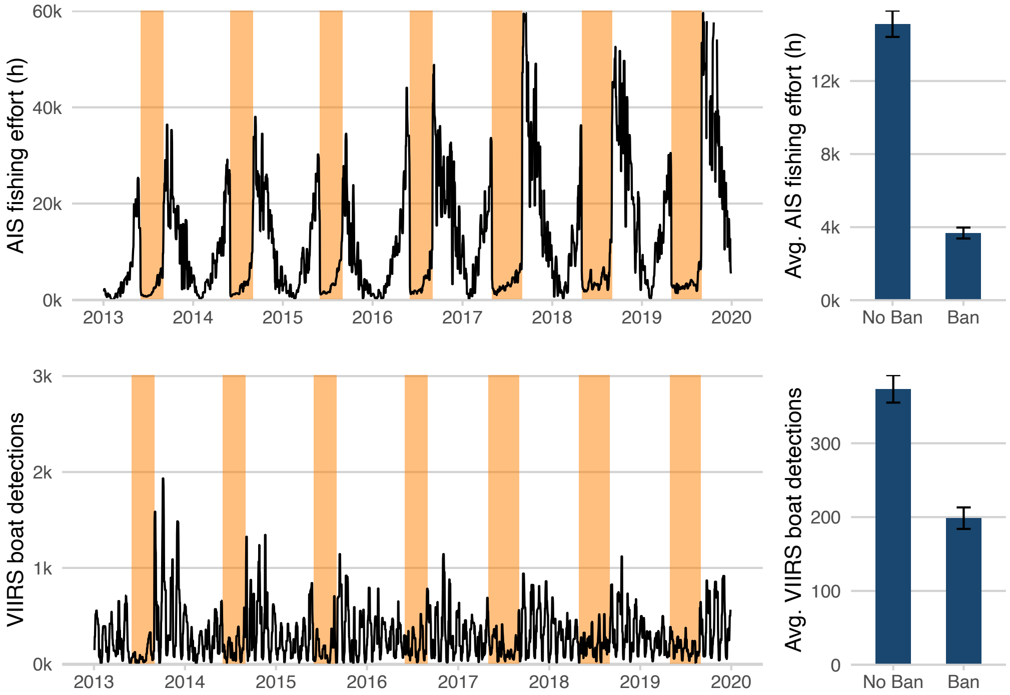

Notes: The left panels show the daily fishing activity indicated by the AIS fishing effort (in hours) and the number of boat detections from satellite images by VIIRS in the North Yellow Sea. Yellow areas indicate times when the fishing ban was in place. The right panels show the average fishing activity for both fishing measures during times without [with] the fishing ban in place. Both time-series have been smoothed and show the rolling median fishing effort in a centered 5 day window. Error bars indicate two standard errors. Note that a simple comparison of the average level of fishing activity between both periods does not reflect the reduction due to the ban as it does not consider the counterfactual level of fishing activity during the ban.

Table 1: Descriptive statistics by management zone

	Zone 1	Zone 2	Zone 3	Zone 4
AIS vessels hours	28,539.19	24,122.01	18,449.79	8,505.85
AIS fishing effort (hours)	11,797.95	9,529.45	7,680.13	4,148.60
Gear type (AIS)				
Trawelers (%)	0.48	0.44	0.53	0.67
Fixed gear (%)	0.28	0.27	0.31	0.18
Unknown (%)	0.21	0.27	0.12	0.11
Dredge (%)	0.02	0.01	0.02	0.02
Other (%)	0.01	0.02	0.02	0.03
VIIRS boat detections	322.68	569.96	168.34	468.93
Fishing ban	0.29	0.33	0.25	0.25
Moon illumination (lux)	0.02	0.03	0.03	0.03
Weather conditions				
Air temperature (°C)	14.25	18.89	24.38	26.27
Humitidy (g/kg)	8.75	11.79	15.98	17.40
Wind speed (m/s)	6.45	7.06	7.46	6.59
Environmental conditions				
Sea surface temperature (°C)	14.47	19.20	23.63	26.78
Chlorophyll-a (mg/m3)	2.80	2.04	1.56	0.67
Phytopl. absorpt. coef. (×100, Aph)	0.50	0.64	0.68	0.68
Observations	2556	2556	2556	2556

Notes: The Table shows mean values of the zone sample. Each observation refers to one day. Data ranges from January 2013 to December 2019. The underlying gear types of the AIS fishing effort data are inferred by vessel movements (Kroodsma et al. 2018). For additional descriptive statistics including the grid sample please refer to Table A6 in the Appendix.

Figure 4: Reduction in fishing activity due to the ban per management zone

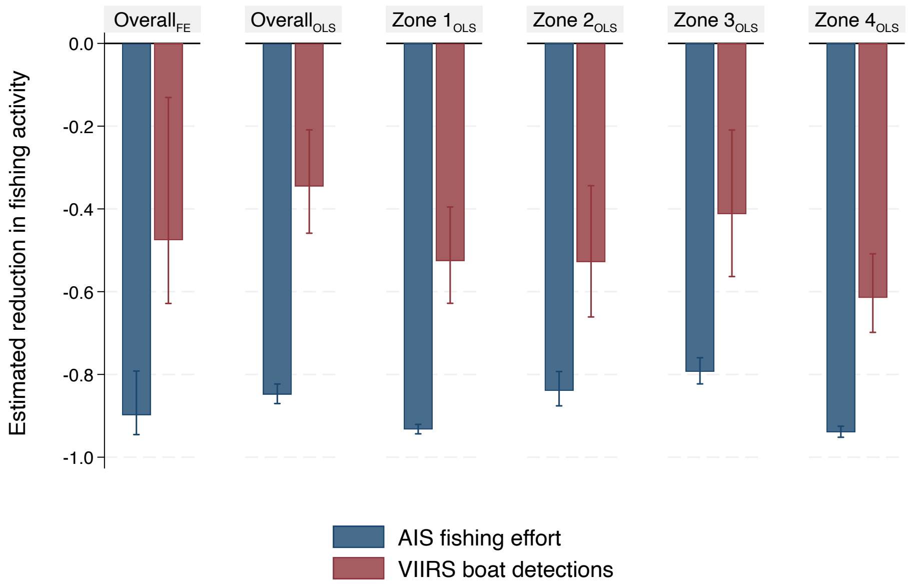

Notes: The figure shows the estimated reduction in fishing activity based on Equation (1) for the whole Chinese EEZ and each management zone. The graph shows the estimated coefficients and 95 percent confidence intervals that have been transformed to indicate exact percentage changes. For more detailed results, see Table A8 in the Appendix.

Figure 5: Locations with apparent fishing activity during the ban

(a) AIS fishing effort (b) VIIRS boat detections

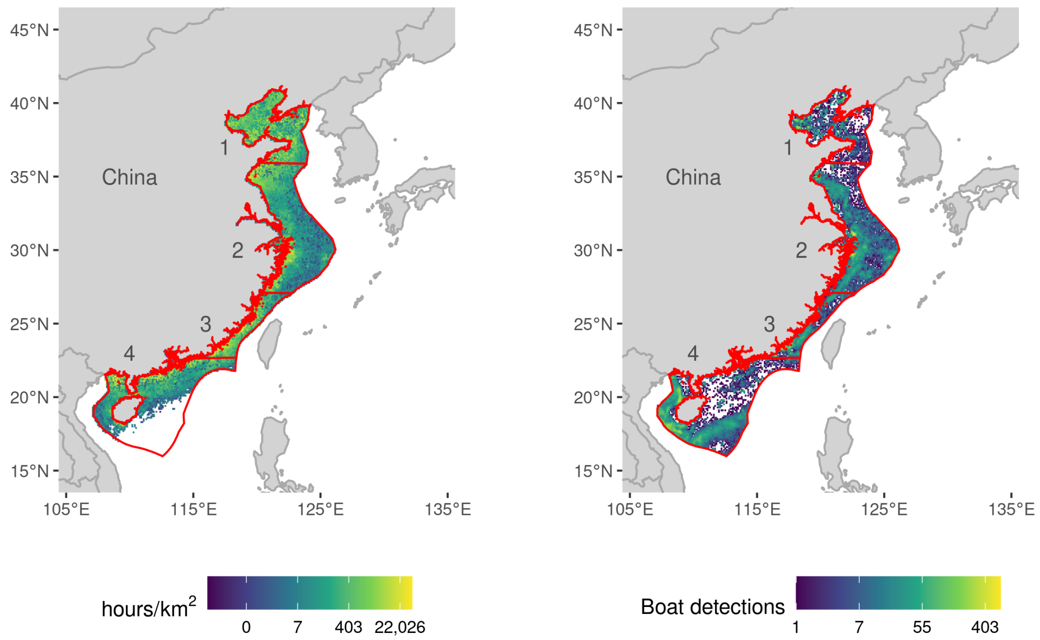

Notes: Both maps show the location and total level of fishing activity during the ban periods from 2013 to 2019. Subfigure (A) shows the sum of the AIS fishing effort and Subfigure (B) shows the sum of VIIRS boat detections during that time. The red areas and gray numbers indicate the respective management zones within the Chinese EEZ.

Table 2: Effect of good fishing conditions on compliance with the ban

	Occurrence of fishing activity		Level of fishing activity	
	AIS	VIIRS	AIS	VIIRS
	(1)	(2)	(3)	(4)
Phytoplankton	-0.006**	0.011***	-0.007	0.011
	(0.003)	(0.003)	(0.015)	(0.008)
Ban	-0.083***	-0.039**	-0.794***	-0.187***
	(0.019)	(0.014)	(0.092)	(0.054)
Phytoplankton × Ban	0.032***	0.052***	0.181***	0.162***
	(0.005)	(0.005)	(0.030)	(0.017)
Observations	309,695	309,695	128,900	183,135
Mean of dep. var. (no ban)	0.44	0.62	4.66	1.79

Notes: Fixed effects estimation for the grid sample. In Column (1) and (2), the dependent variables are dummy variables equal to one if AIS fishing effort [VIIRS boat detections] occur in a given grid-cell in a given week and they are zero otherwise. In Columns (3) and (4), dependent variables are the logarithm of the respective fishing effort measures. In all regressions we consider the standardized phytoplankton abundance (z-score). Additional covariates include week-year fixed effects and cell fixed effects. Conley (1999, 2008) standard errors are shown in parentheses and correct for spatial auto-correlation. * $p < 0.1$, ** $p < 0.05$, *** $p < 0.001$